EGEE 520

Selective Catalytic Reduction (SCR) of NO by NH_3 in a Fixed-bed Reactor

Hee Je Seong

1. Introduction

Fossil fuels have been main sources for energy in terms of combustion, where chemical energy in fuels is converted into thermal and mechanical energies. When air reacts with fuels at high temperature, NOx representing NO, NO_2, N_2O, N_2O_5 and etc is unavoidable due to the reaction between oxygen and nitrogen in air [1, 2]. NOx is toxic as itself as well as a precursor of acid rain, so its regulation has been becoming more stringent all over the countries. There has been much interest in reducing NOx from engines in terms of fuel injection strategies [3], exhaust gas recirculation [4] and catalytic reactions [5], among which selective catalytic reduction (SCR) has been successfully applied in stationary applications such as boilers and power plants [6]. Although there are many reducing agents suggested, gaseous ammonia shows the best performance for this reaction [7]:

$$4NH_3 + 4NO + O_2 \rightarrow 4N_2 + 6H_2O \qquad (1.1)$$

Although the equation (1.1) is a major pathway for NO in the presence of O_2, the equation (1.2) is also important when NO_2 is high in the mixture of NO and NO_2 [8].

$$4NH_3 + 2NO + 2NO_2 \rightarrow 4N_2 + 6H_2O \qquad (1.2)$$

There have been many catalysts developed for the SCR reaction [9, 10], among which a V_2O_5/TiO_2 catalyst has been widely used in commercial applications [10]. Although the equation (1.1) is an overall reaction for SCR, many elementary steps are involved during the reaction between NO and NH_3 [11]. Since NO is reacted with NH_3 on catalysts, its detailed reaction mechanism has been of great interest in order to develop kinetic models of SCR depending upon catalysts [12 – 14]. According to many studies, it is accepted that NO is reacted via the Langmuir-Hinshelwood mechanism in V_2O_5-WO_3/TiO_2 catalysts [13], where gaseous NO and NH_3 are adsorbed on the catalysts and adsorbed NO and NH_3 are reacted on the surface.

There have been many researches for modeling of ammonia-SCR systems [15 - 19]. As evidenced by experiments, oxygen concentration in the exhaust gases is crucial for the SCR. Therefore, some kinetic models took into account the oxygen concentration [18, 19]. However, Chae et al. only considered NO and NH_3 concentrations for their model although oxygen effect was already employed in their model [16]. Another important parameter in the SCR model is whether NH_3 is oxidized by reacting oxygen as shown in the equation (1.3) [17, 18]. Since this reaction is active at high temperature over 400^oC, it is observed that NO removal activity decreases over this temperature because NH_3 which needs for NO reaction is converted into NO.

$$4NH_3 + 5O_2 \rightarrow 4NO + 6H_2O \qquad (1.3)$$

In this study, the reaction between NO and NH_3 was simulated in COMSOL using fundamental mass and momentum equations. The model was studied if it is appropriate to describe SCR reaction, which has been experimentally proven.

2. Governing Equations

There are two governing equations employed in this model; one is a mass equation, and the other is a momentum equation. Although there is a heat evolved during the reaction of NO and NH_3, an energy equation was not considered because it is very small due to small amounts of two reactants. The equation (2.1) indicates a mass equation in an advective flow.

$$A\frac{\partial c}{\partial t} + \nabla \cdot (-D\nabla c) = R - \boldsymbol{v} \cdot \nabla c \qquad (2.1)$$

where c is a concentration, D is a diffusion coefficient, R is a chemical reaction, and **v** is a velocity which is a vector form. Since the mass equation is assumed at a steady state, the 1st term is canceled out and finally the equation becomes the equation (2.2)

$$\nabla \cdot (-D\nabla c) = R - \boldsymbol{v} \cdot \nabla c \qquad (2.2)$$

For a momentum equation, the incompressible Navier-Stokes equation in a laminar flow was employed as shown in the equation (2.3) and (2.4)

$$\rho\frac{\partial \boldsymbol{v}}{\partial t} + \rho(\boldsymbol{v} \cdot \nabla)\boldsymbol{v} = F - \nabla p + \eta\nabla^2\boldsymbol{v} \qquad (2.3)$$

$$\nabla \cdot \boldsymbol{v} = 0 \qquad (2.4)$$

where ρ is a density, F is a convective force, p is a pressure, and η is a dynamic viscosity.

Since there is no convective force and the intertial force is assumed negligible, then the equation (2.3) becomes as follows.

$$\rho(\boldsymbol{v} \cdot \nabla)\boldsymbol{v} = -\nabla p + \eta\nabla^2\boldsymbol{v} \qquad (2.5)$$

3. Formulation

The reaction of NO and NH_3 was simulated in 2-D according to Fig. 3.1, where the box is a cross-section in the center of the tubular reactor. The boundary conditions are also given in the figure.

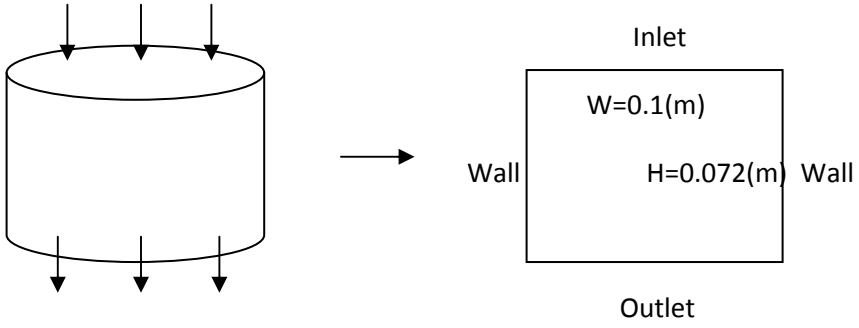

Fig. 3.1 Model for the simulation and its boundary condition

The mass equation (2.2) is used directly in this model and the reaction rates of NO and NH_3 are given in (3.1) – (3.5) referring to Chae et al.'s kinetic model [16] because it includes the reaction kinetics and related kinetic constants with their experimental and simulated results. The kinetic constants employed in this model are tabulated in Table 3.1 as well.

$$-r_{NO} = \frac{k_{NO}K_{NH3}C_{NO}C_{NH3}}{1+K_{NH3}C_{NH3}} - \frac{k_{NH3}K_{NH3}C_{NH3}}{1+K_{NH3}C_{NH3}} \quad (3.1)$$

$$-r_{NH3} = \frac{k_{NO}K_{NH3}C_{NO}C_{NH3}}{1+K_{NH3}C_{NH3}} + \frac{k_{NH3}K_{NH3}C_{NH3}}{1+K_{NH3}C_{NH3}} \quad (3.2)$$

$$\text{where } k_{NO} = k_{NO}^{o}\exp\left(-\frac{E_{NO}}{RT}\right) \quad (3.3)$$

$$k_{NH3} = k_{NH3}^{o}\exp\left(-\frac{E_{NH3}}{RT}\right) \quad (3.4)$$

$$K_{NH3} = K_{NH3}^{o}\exp\left(\frac{H_{NH3}}{RT}\right) \quad (3.5)$$

Table 3.1 Kinetic parameters at the given reaction rates

Kinetic parameters	Values	Name
E_{NO} (kcal/mol)	11.5	Enthalpy of NO reduction
E_{NH3} (kcal/mol)	42.8	Enthalpy of NH_3 oxidation
H_{NH3} (kcal/mol)	21.5	Heat of adsorption of NH_3
k_{NO}^{o} (1/s)	$2.79\text{x}10^{6}$	Collision factor for NO reduction
k_{NH3}^{o} (mol/cm^{3}s)	$6.38\text{x}10^{5}$	Collision factor for NH_3 oxidation
K_{NH3}^{o} (cm^3/mol)	59.6	Equilibrium constant of NH_3 adsorption

The equation (2.5) was also used for the momentum equation in this model, but it is corrected for the model taking into account Brinkman equation as shown in (3.6) since the reactor simulated in the model is porous.

$$\left(\eta/\kappa\right)\boldsymbol{v} = -\nabla p + \frac{1}{\varepsilon}\eta\nabla^2\boldsymbol{v} \quad (3.6)$$

where ε is a porosity of the reactor and κ is a permeability.

In the Chae et al.'s model, the porosity of the reactor is not available, so there is no information available for permeability and pressure drop across the reactor. Accordingly, pressure drop and permeability were calculated using Ergun's equation and Darcy's law, respectively, as indicated in (3.7) and (3.8).

$$\frac{\Delta p}{L} = \frac{150\eta(1-\varepsilon)^2 v}{d_p^2\varepsilon^3} + \frac{1.75\rho(1-\varepsilon)v^2}{d_p\varepsilon^3} \quad (3.7)$$

Where L is a reactor length, d_p is a particle diameter, and ρ is a density of the fluid.

$$Q = \frac{\kappa A}{\eta}\frac{\Delta p}{L} \quad (3.8)$$

where Q is a flow rate through the reactor and A is a cross-sectional area of the flow.

The fluid flowing through the reactor is assumed as air because it is not much different from the exhaust gases in real plants and its properties at different temperatures are available in Turns' book [2]. Since the density and the dynamic viscosity of air are temperature-dependent, their values were plotted as a function of temperature as shown in Fig. 3.2. From the fitted equations, the density and the dynamic viscosity are given as a function of temperature and the equations were used for the calculation of pressure drop and permeability in (3.7) and (3.8).

$$\rho = 9.66 \times 10^{-10} T^{1.7} \tag{3.9}$$

$$\eta = \frac{3.49 \times 10^{2}}{T} \tag{3.10}$$

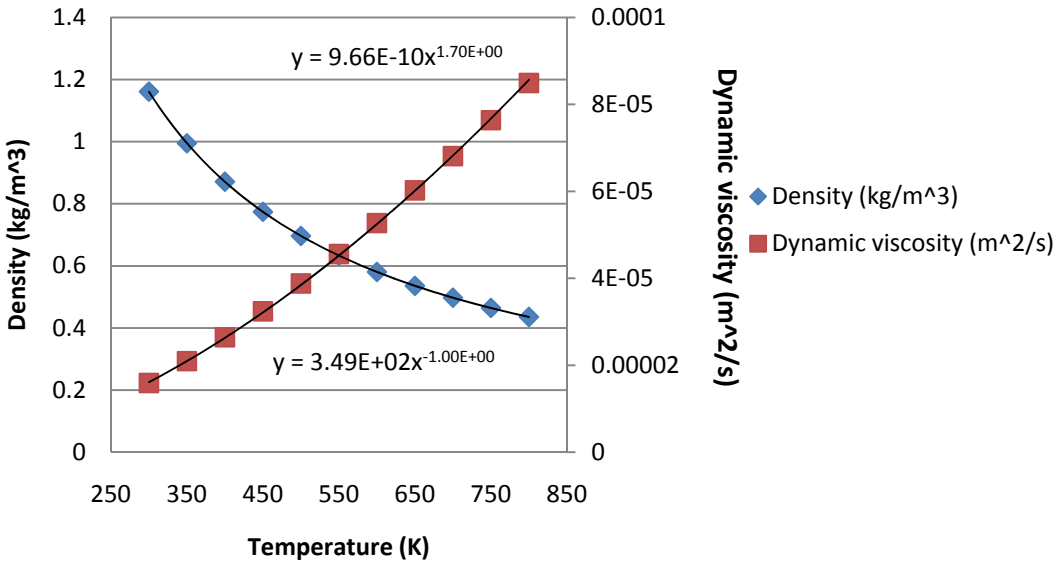

Fig. 3.2 Density and dynamic viscosity of air

4. Solution

The COMSOL model was simulated using the formulation explained in the previous section, and the result is like Fig. 4.1.

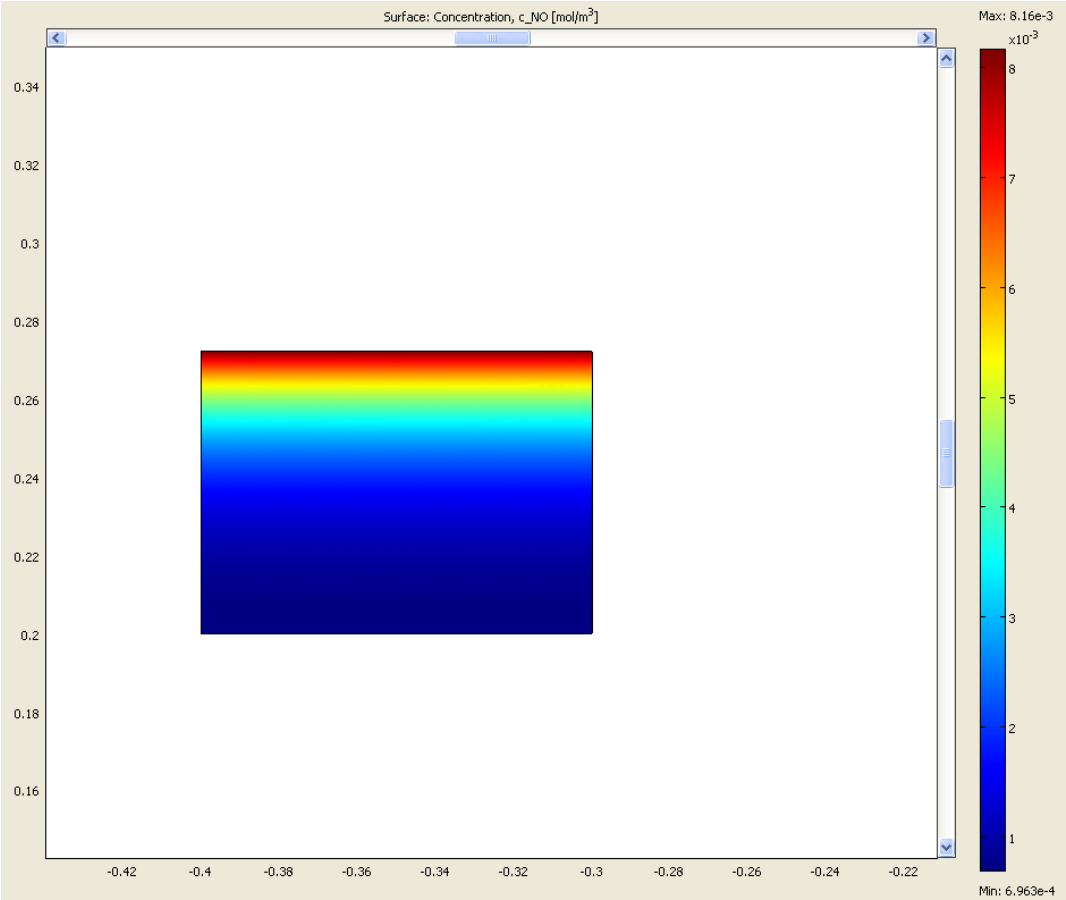

Fig. 4.1 NO concentration distribution on the bed

It shows that much portion of the initial NO concentration is consumed in the inlet of the reactor. In order to understand how the NO and NH_3 concentrations change as gases flow through the reactor, they are plotted along the center line of the reactor as shown in Fig. 4.2.

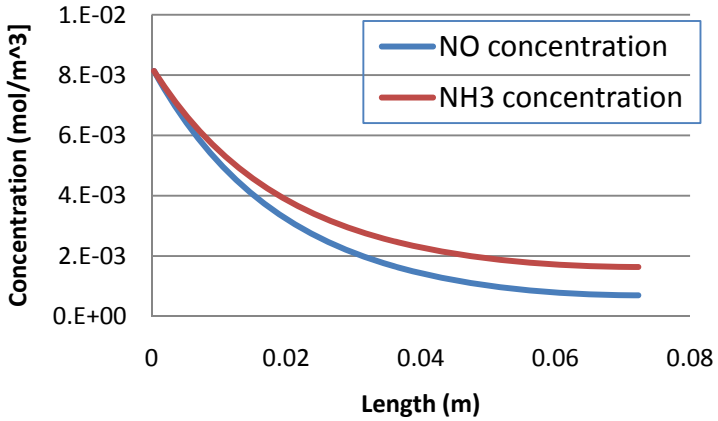

Fig. 4.2 NO and NH_3 concentrations along the center line in the reactor

The figure displays that NO consumption is faster than that of NH_3, and the half of the initial NO concentration is consumed at 0.015 m. At this velocity of 1m/s, the NO and NH_3 removal efficiencies at the exit is almost 91.4% and 80%, respectively. Since the NH_3 slip is also regulated in the emissions, the result indicates that NH_3 concentration should be less than NO concentration. In the parametric study, the various NH_3 concentrations were employed to understand the effect of the initial NH_3 concentration on the NO removal performance.

5. Validation

In order to validate the COMSOL model employed in this simulation, Chae et al.'s results were compared in Fig. 5.1 for 100,000 h^{-1} and 200,000 h^{-1}.

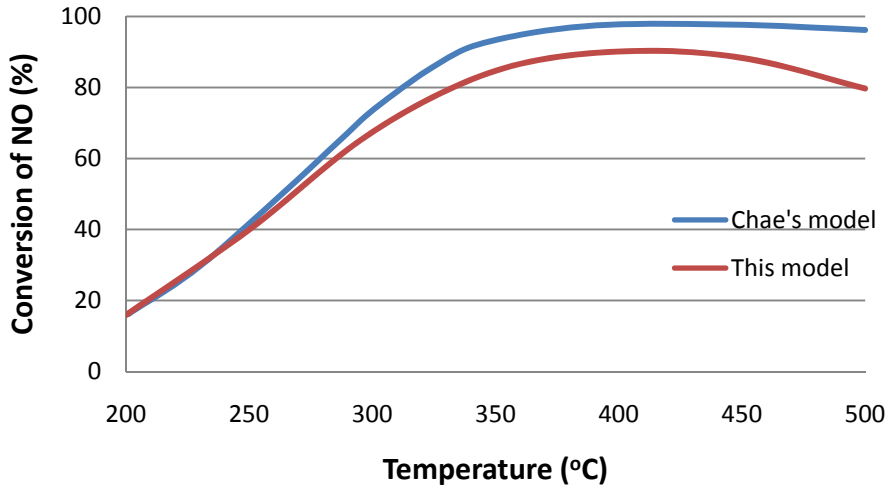

(a) Space velocity = 100,000 h^{-1}

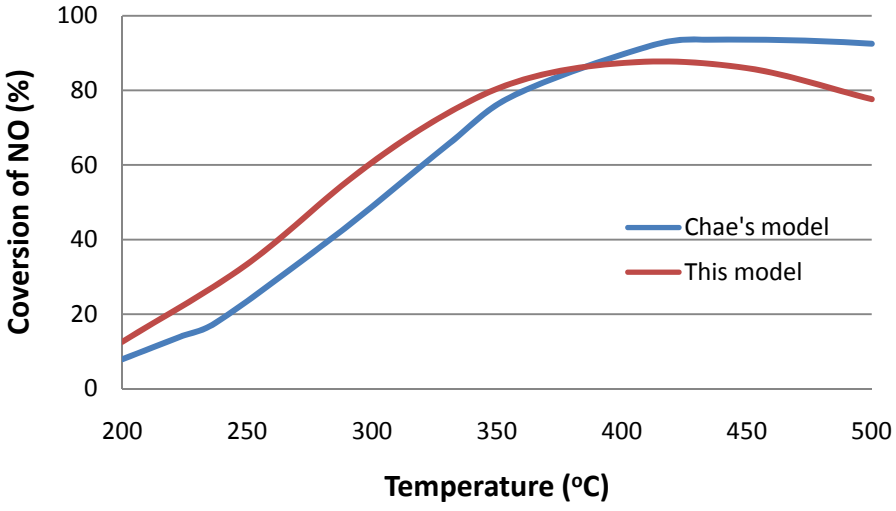

(b) Space velocity = 200,000 h^{-1}

Fig. 4.1 Comparison of Chae et al.'s model and the COMSOL model

As shown in the figures, the COMSOL model well depicts the trends of Chae et al.'s results in the conversion of NO as a function of temperature for two space velocities. However, the results by the COMSOL model are found to be not the same as Chae et al.'s model in spite of the same kinetic reactions. Since the paper didn't include any detailed information about the model conducted in their calculation except the kinetic data for NO and NH_3 consumptions, there might be the difference in the results between two models. Taking into account the limitation of the COMSOL model to predict Chae et al's result, the model appears to be useful to evaluate the kinetic simulation of NO and NH_3 reaction. Accordingly, the parametric study was also conducted using this model in the following section to find the effect of various parameters such as NH_3-NO ratio and pressure drop in the catalytic bed on the reaction.

6. Parametric Study

In this session, three parametric studies were employed; NH_3/NO effect, porosity effect and water effect.

As discussed in the solution part, the consumption of NH_3 through the catalytic reactor is not the same as that of NO. Therefore, NH_3/NO needs to be controlled to minimize NH_3 slip with keeping high NO removal reactivity. As shown in Fig. 6.1, conversion of NO was tested for NH_3/NO of 0.85, 1 and 1.15 as a function of temperature. The figure indicates that there is no variation in the conversion of NO up to 350°C with changing the ratio and the conversion increases with the increase in the ratio above the temperature. And, the result also shows that above 400°C, the conversion is increased by 4 – 6.5% for the ratio of 1 with respect to 0.85 and it is increased by 2 – 4.5% for the ratio of 1.15 with respect to 1. Consequently, the effect of increased NH_3/NO is not significant for the ratio of 1.15. Accordingly, it is concluded that NH_3/NO should be less than 1 below 350°C and it should be controlled taking account of the conversion above 400°C if there is NH_3 slip regulated.

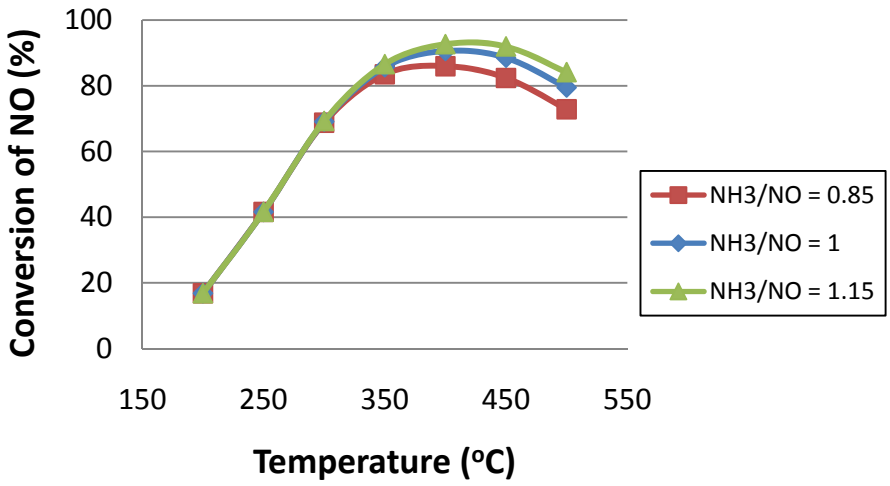

Fig. 6.1 Effect of NH_3/NO on conversion of NO

According to Chae et al.'s paper, the porosity of a V_2O_5-WO_3/TiO_2 catalyst used in their experiment is 0.38, but there is no additional information about the porosity of their catalytic reactor. Since the porosity of the reactor affects permeability and pressure drop in this model significantly, NO removal activity is also compared for the porosity of 0.5 and 0.7 as shown in Fig. 6.2. In spite of obvious changes in permeability and pressure drop displayed in Table 6.1, there is no change observed in the conversion of NO. Therefore, the effect of permeability and pressure drop used in this simulation on the kinetics seems to be negligible.

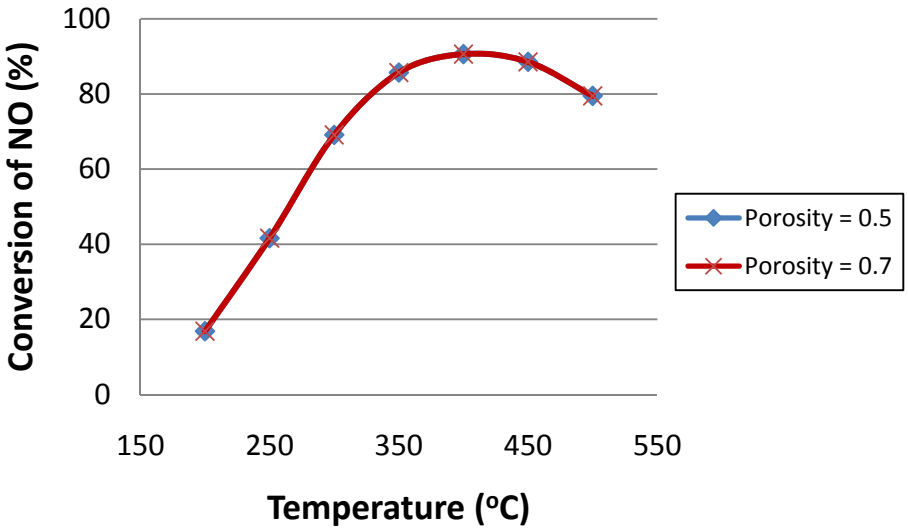

Fig. 6.2 Effect of porosity in a reactor bed on conversion of NO

Table 6.1 Permeability and Pressure drop for the porosity of 0.5 and 0.7

Temperature (°C)	Porosity = 0.5		Porosity = 0.7	
	ΔP (Pa)	K (m^2)	ΔP (Pa)	K (m^2)
200	29492	$3.33x10^{-10}$	4390	$2.23x10^{-9}$
250	33308	$3.49x10^{-10}$	4861	$2.40x10^{-9}$
300	37529	$3.62x10^{-10}$	5353	$2.54x10^{-9}$
350	42119	$3.72x10^{-10}$	5921	$2.65x10^{-9}$
400	47057	3.80x10-^{10}	6539	$2.73x10^{-9}$
450	52323	$3.86x10^{-10}$	7205	$2.80x10^{-9}$
500	57901	$3.90x10^{-10}$	7915	$2.86x10^{-9}$

Water effect on NH_3 SCR is known to be significant due to the competition between H_2O and NH_3 in order to adsorb on active sites of a catalyst [20]. Since kinetic parameters at wet condition are also available in Chae et al.'s paper, they are compared in Table 6.2 and the conversion of NO is compared for wet and dry conditions in Fig. 6.3. As discussed in the Dumesic et al.'s paper [20], it is

clearly observed that NO removal activity is hindered by H_2O below 400°C, but it appears that the activity is even increased above the temperature because higher temperature enables to overcome higher activation energies of NO and NH_3. Consequently, the wet condition is better to operate at high temperature in order to reach higher NO removal activity. Since water is contained in the exhaust gases from actual plants, the model at wet condition will be more realistic in order to evaluate the performance of this catalytic reactor.

Table 6.2 Comparison of kinetic parameters at dry and wet conditions

Kinetic parameters	Dry condition	Wet condition
E_{NO} (kcal/mol)	11.5	12.1
E_{NH3} (kcal/mol)	42.8	57.6
H_{NH3} (kcal/mol)	21.5	22.2
k_{NO}^{o} (1/s)	2.79×10^{6}	3.04×10^{6}
k_{NH3}^{o} (mol/cm^{3}s)	6.38×10^{5}	9.98×10^{8}
K_{NH3}^{o} (cm^3/mol)	59.6	69.1

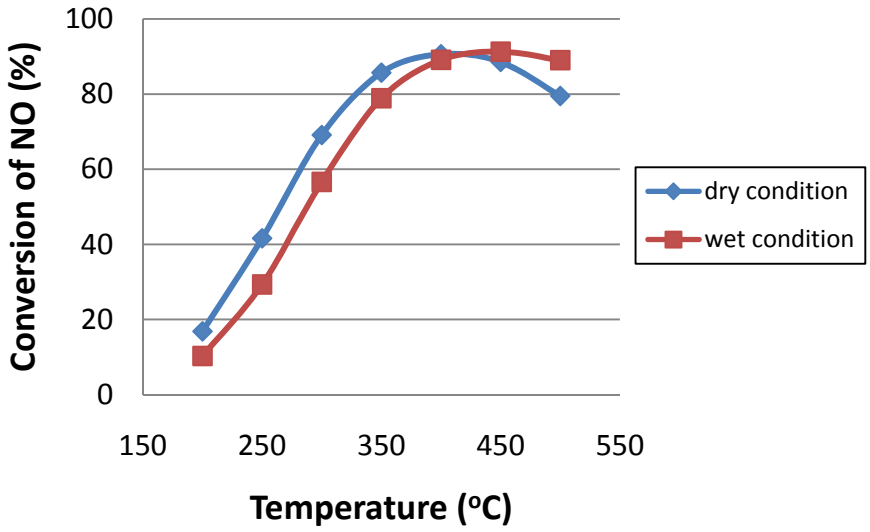

Fig. 6.3 Comparison of NO conversions at dry and wet conditions

Conclusion

NOx emissions from engines, incinerator and power plants are one of the most problematic pollutants. Since it is well-known that NOx in the exhaust gases is effectively removed by NH_3 in a catalytic reactor, which is called selective catalytic reduction (SCR), a catalytic fixed-bed reactor was simulated in 2-D using COMSOL for the reaction. The model well describes the trend of NO removal with respect to temperature when it is compared to Chae et al.'s kinetic model. It is shown that much of NO concentration is consumed in the inlet of the reactor, and the NO consumption rate is slightly higher than that of NH_3. When the ratio of NO and NH_3 is varied, the model displays that with the increasing

ratio, there is no increase in the conversion of NO below 350^{o}C. And, there is a slight increase above 400^{o}C when the ratio is beyond 1, so the ratio should be controlled taking into account NH_3 slip and NO conversion at specific temperatures. The model also shows that there is no effect on the conversion with different porosities in the reactor even though pressure drop and permeability through the reactor are dependent much on the porosity. When the kinetic model was calculated for dry and wet conditions, the model also clearly indicates that NO conversion is lowered below 400^{o}C at wet condition, resulted from the inhibition of NH_3 adsorption onto active sites by water at low temperatures. Accordingly, it is concluded that the COMSOL model can be usefully employed to understand NO and NH_3 reaction in this catalytic reactor.

References

1. Whitty, K. J., Zhang, H. R., and Eddings, E. G., "Emissions from syngas combustion", Combust. Sci. and Tech., Vol. 180, p. 1117 – 1136, 2008
2. Turns, S. R., "An introduction to combustion: concepts and applications", 2nd edition, McGraw Hill, p. 559 – 567, 2000
3. Boehman, A. L. Morris. D., and Szybist, J., "The impact of the bulk modulus of diesel fuels on fuel injection timing", Energy & Fuels, Vol. 18, p. 1877 – 1882, 2004
4. Abd-Alla, G. H., "Using Exhaust Gas Recirculation in Internal Combustion Engines: A Review", Energy Conversion and Management, Vol. 43, p. 1027 – 1042, 2002
5. Traa, Y., Burger, B., and Weitkamp, J., "Zeolite-based materials for the selective catalytic reduction of NOx with hydrocarbons", Microporous and Mesoporous Materials, Vol. 30, p. 3 – 41, 1999
6. Heck, R. M., "Catalytic abatement of nitrogen oxides–stationary applications", Catalysis Today, Vol. 53, p. 519 – 523, 1999
7. Koebel, M., and Strutz, E. O., "Thermal and hydrolytic decomposition of urea for automotive selective catalytic reduction systems: thermochemical and practical aspects, Ind. Eng. Chem. Res., Vol. 42, p. 2093 – 2100, 2003
8. Devadas, M., Kröcher, O., Elsener, M., Wokaun, A., Söger, N., Pfeifer, M., Demel, Y., and Mussmann, L., "Influence of NO_2 on the selective catalytic reduction of NO with ammonia over Fe-ZSM5", Applied Catalysis B: Environmental, Vol. 67, p. 187 – 196, 2006
9. Brandenberger, S., Kröcher, O., Tissler, A., and Althoff, R., "The state of the art in selective catalytic reduction of NOx by ammonia using metal-exchanged zeolite catalysts", Catalysis Reviews, Vol. 50, p. 492 – 531, 2008
10. Heck, R. M., "Catalytic abatement of nitrogen oxides–stationary applications", Catalysis Today, Vol. 53, p. 519 – 523, 1999
11. Topsoe, N. Y., Topsoe, H., and Dumesic, J. A., "Vanadia/titania catalysts for selective catalytic reduction (SCR) of nitric-oxide by ammonia: I. Combined temperature-programmed in-situ FTIR and on-line mass-spectroscopy studies", Journal of Catalysis, Vol. 151, p. 226 – 240, 1995
12. Muñiz, J., Marbán, G., and Fuertes, A. B., "Low temperature selective catalytic reduction of NO over modified activated carbon fibres", Applied Catalysis B: Environmental, Vol. 27, p. 27 – 36, 2000
13. Koebel, M., and Elsener, M., "Selective catalytic reduction of NO over commercial DeNOx-catalysts: experimental determination of kinetic and thermodynamic parameters", Chemical Engineering Science, Vol. 53, p. 657 – 669, 1998

14. Kijlstra, W. S., Brands, D. S., Smit, H. I., Poels, E. K., and Bliek, A., “Mechanism of the selective catalytic reduction of NO with NH3 over MnOx/Al2O3: II. Reactivity of adsorbed NH3 and NO complexes”, Journal of Catalysis, Vol. 171, p. 219 – 230, 1997
15. Roduit, B., Wokaun, A., and Baiker, A., “Global Kinetic Modeling of Reactions occurring during selective catalytic reduction of NO by NH3 over vanadia/titania-based catalysts”, Ind. Eng. Chem. Res., Vol. 37, p. 4577 – 4590, 1998
16. Chae, H. J., Choo, S. T., Choi, H., Nam, I., Yang, H. S., and Song, S. L., “Direct use of kinetic parameters for modeling and simulation of a selective catalytic reduction process”, Ind. Eng. Chem. Res., Vol. 39, p. 1159 – 1170, 2000
17. Cho, J. M., Choi, J. W., Hong, S. H., Kim, K. C., Na, J. H., and Lee, J. Y., “The methodology to improve the performance of a selective catalytic reduction system installed in HRSG using computational fluid dynamics analysis, ENVIRONMENTAL ENGINEERING SCIENCE, Vol. 23, p. 863 – 873, 2006
18. Tsinoglou, D., and Koltsakis, G., “Modeling of the selective catalytic NOx reduction in diesel exhaust including ammonia storage”, Proc. IMechE: J. Automobile Engineering, Vol. 221, p. 117 – 133, 2007
19. Zürcher, S., Hackel, M., and Schaub, G., “Kinetics of selective catalytic NOx reduction in a novel gas-particle filter reactor (catalytic filter element and sponge insert)”, Ind. Eng. Chem. Res., Vol. 47, p. 1435 – 1442, 2008
20. Dumesic, J. A., Topsøe, N. –Y., Topsøe, H., Chen, Y., and Slabiak, T., “Kinetics of selective catalytic reduction of nitric oxide by ammonia over vanadia/titania”, Journal of catalysis, Vol. 163, p. 409 – 417, 1996